(4)

Carderock Division
Naval Surface Warfare Center
Bethesda, Md. 20084-5000

CRDKNSWC-SSM-64-92/22 April 1993

Survivability, Structures, and Materials Directorate
Technical Report

Measurement of the Out-of-Plane Shear Response of Thick Section Composite Materials Using the V-notched Beam Specimen

by
K. Gipple
D. Hoyns

45pg

CRDKNSWC-SSM-64-92/22 Measurement of the Out-of-Plane Shear Response of Thick Section Composite Materials Using the V-notched Beam Specimen

Carderock Division
Naval Surface Warfare Center
Bethesda, Md. 20084–5000

CRDKNSWC–SSM–64—92/22 April 1993
Survivability, Structures, and Materials Directorate
Technical Report

Measurement of the Out-of-Plane Shear Response of Thick Section Composite Materials Using the V-notched Beam Specimen

by
K. Gipple
D. Hoyns

Approved for public release; distribution is unlimited.

TABLE OF CONTENTS

LIST OF TABLES

LIST OF FIGURES

ABSTRACT

The out-of-plane shear response of thick, unidirectional and crossply, AS4/3501-6 and S2 glass/3501-6 laminates was investigated theoretically and experimentally. The specimens considered were of the V-notched beam (Iosipescu) configuration. Strains were monitored in the specimen test sections using conventional strain gages, moiré interferometry and new full section strain gages. Crossply laminates exhibited a fairly uniform strain distribution away from the notches resulting in agreement of initial moduli obtained through all three strain measurement methods. Strains measured with conventional gages centered between the notches of the unidirectional specimens exceeded the average strain from notch to notch, as measured by moiré interferometry and the full section gages. Therefore, a lower initial modulus was calculated using conventional gage data vs. moiré or full section data. Measured strains correlated very well with predicted strains from specimen finite element analyses using nonlinear elastic material properties.

ADMINISTRATIVE INFORMATION

This program was supported by the CDNSWC Materials Block Program Office, sponsored by ONT and administered by Ivan Caplan (0115) under Work Unit 1-2802-601-10. Material modeling and analysis efforts were supported by the CDNSWC IR/IED Program Office, sponsored by ONR and administered by Dr. Bruce Douglas (0113), under Work Units 1-2844-220 and 1-2844-240.

INTRODUCTION

Increasing the efficiency of composite designs requires a better understanding of the three-dimensional (3-D) behavior of composite materials. Of particular interest is the out-of-plane or through-thickness direction. The combination of through-thickness shear and tensile stresses with the inherently low through-thickness strength of composite materials plays a vital role in composite structural behavior [1-6]. At some geometric discontinuities such as free edges or ply dropoff regions, through-thickness stresses can be minimized by careful choice of lamina stacking sequence [7] or proper design procedures [3]. However, in many

instances, the significance of through-thickness stresses must be assessed on a case by case basis due to fixed laminate or geometry requirements [3]. Three dimensional analyses of structures or structural details dominated by through-thickness stresses are also complicated by the scarcity of through-thickness material data due to the lack of suitable specimens to measure out-of-plane behavior [5,8].

The current study focuses on the measurement of the through-thickness shear response using the V-notched beam (Iosipescu) specimen in the modified Wyoming test fixture [9]. The V-notched beam specimen is typically used for in-plane shear testing of composites. It has been rigorously investigated with regards to specimen geometry and loading effects [10], plasticity and material orientation effects [11], strain field uniformity and purity [10], and repeatability of results [12]. Adams et al. [13] did use the V-notched beam specimen for through-thickness shear measurements comparing the behavior of unidirectional and cross-ply laminates fabricated by bonding several thin laminates together vs. those cut from a single thick laminate. To the authors' knowledge, no study has investigated the use of the Iosipescu specimen for through-thickness shear testing more throroughly.

In this program, moiré interferometry and 3-D finite element analyses (3-D elastic and 3-D nonlinear elastic material properties) are used to evaluate the uniformity and purity of the strain field in the gage section of the through-thickness shear V-notched beam specimen. The impact of nonuniform fields on strain gage measurements is also discussed. The results from an experimental gage developed at the Virginia Polytechnic Institute and State University (VPI&SU) [14] are included for comparison to conventional gages and to assess the differences in average strain readings between the front and the back of the specimen.

BACKGROUND: MOIRÉ INTERFEROMETRY

High sensitivity moiré interferometry is an optical technique for whole field deformation measurement. In this study, a collimated beam of light was directed to a three mirror interferometer (Figure 1) producing two orthogonal virtual reference gratings of frequency f [15]. These gratings interact with a cross-lined diffraction grating of frequency f/2, replicated

onto the specimen surface, to create contour maps of U (horizontal) and V (vertical) displacement fields. These contour maps are composed of alternating black and white fringe patterns. The surface normal strains, ε_x and ε_y, and shear strain, γ_{xy}, are related to the displacement fields by the equations:

$$\varepsilon_x = \frac{\partial U}{\partial x} = \frac{1}{f}\left(\frac{\partial N_x}{\partial x}\right) \tag{1}$$

$$\varepsilon_y = \frac{\partial V}{\partial y} = \frac{1}{f}\left(\frac{\partial N_y}{\partial y}\right) \tag{2}$$

$$\gamma_{xy} = \frac{\partial U}{\partial y} + \frac{\partial V}{\partial x} = \frac{1}{f}\left[\frac{\partial N_x}{\partial y} + \frac{\partial N_y}{\partial x}\right] \tag{3}$$

where N_x and N_y correspond to the U and V field fringe order, respectively.

EXPERIMENTAL

Materials and Specimen Preparation

The material systems evaluated in this investigation were Hercules AS4/3501-6 graphite/epoxy and S2/3501-6 glass/epoxy prepreg. Thick-section panels of unidirectional $[0]_{140}$ and crossply $[0/90]_{72S}$ construction were fabricated and autoclave cured at CARDEROCKDIV, NSWC. As specified in Figure 2, V-notched beam specimens were machined from the unidirectional panels in the 90° direction, and will be referred to as the G_{23} specimens. Specimens from the crossply panel were machined in the 0° and 90° directions to obtain G_{xz} and G_{yz}. Unidirectional AS4 specimens were 0.51 cm. (0.20 in.) thick, unidirectional S2 glass specimens were 0.38 cm. (0.15 in.) thick, and crossply specimens of both materials were 0.53 cm. (0.21 in.) thick. Fiber volumes were determined by standard matrix digestion and incineration methods, ASTM D3171 [16] and ASTM D2584 [17] respectively. Specimen surfaces were ground and polished with 1200

micron grit paper using standard metallographic techniques.

Instrumentation and Mechanical Testing

Conventional Method

Stacked (0°/90°) strain rosettes (Measurements Group CEA-06-062WT-350) were centered between the notch roots at +45/-45 degrees to the loading axis (Figure 3). Gages were bonded to both the front and back faces of the specimens. Compliant shims were also placed along the edges of the specimens to avoid possible twisting from localized asperities, as reported by Morton, et al. [10]. The CARDEROCKDIV, NSWC V-notched beam test fixture, based on specifications for the modified Wyoming version developed by Walrath and Adams [11], is pictured in Figure 4. Specimens were centered in the fixture and loaded to failure at 1.25 mm/min.(.05 in./min.) by a hydraulic, 267 kN (60,000 lb.) capacity, Satec testing machine. Strain output was conditioned through 2310 amplifiers and recorded by a microcomputer based data acquisition system.

Moiré Interferometry and New Full Section Strain Gage

Specimen gratings approximately 0.0254 mm (0.001 in.) thick were replicated onto the front surface of specimens of each material using the method described in Reference 18. The previously described moiré interferometry system was set up on the cross-head of the test machine and produced a virtual grating frequency of 2400 l/mm (60,960 l/in). The corresponding sensitivity of the displacement measurements is 1/f, or 0.417μm(16.4μin.) per fringe order. The application of gratings and the interferometry testing were performed at VPI&SU.

New full section strain gages with side by side +45°/-45° configuration were developed at VPI&SU and recently made commercially available. One of these gages was bonded to the back surface, opposite the moiré grating, of each of the four specimens. Schematics of the gages used in this study are shown in Figure 3. The loading fixture was of the modified Wyoming type, and the testing machine was a screw-driven 267 kN (60,000 lb.) capacity Tinius Olsen. U and V displacement fields in the test section of the specimens were

recorded on pan film at several load levels, from the clamped no load condition to failure.

Two additional unidirectional (G_{23}) and crossply specimens of each material were also instrumented with back-to-back full section gages. These specimens were tested with the CARDEROCKDIV, NSWC fixture and testing machine referenced previously. Table 1 shows the number of specimens tested for each orientation, material and strain measurement method.

Microscopy

Failed crossply specimens were sputter coated with Au/Pd, then inspected via a JEOL model 35CF scanning electron microscope. Photomicrographs were taken of failure surfaces.

THREE-DIMENSIONAL FINITE ELEMENT ANALYSIS

Finite Element Analysis Program Description

A 3-D finite element analysis of the V-notched beam through-thickness shear coupon was conducted using ABAQUS [19]. ABAQUS is a general purpose finite element program developed by Hibbitt, Karlsson, and Sorensen, Inc. It provides a wide range of options for numerical modeling of structural response. Stress analyses may be static or dynamic, linear or nonlinear. Sources of nonlinearity include material, geometric and boundary condition nonlinearities. A number of nonlinear material models are available in ABAQUS or the material may be described by the user in a UMAT subroutine. The latter option was used in this analysis which considered the effects of both linear and nonlinear elastic material behavior on the response of glass and graphite/epoxy, unidirectional and crossply V-notched beam through-thickness shear specimens.

Nonlinear Material Model

Development of the nonlinear material model used in the analysis followed the framework outlined in Reference 20. This framework consists

of three steps: development of the detailed 3-D nonlinear material response using micromechanical finite element analyses, adjustment of a simplified unit cell material model to match the detailed analysis results, and transition of the simplified model to a general purpose finite element program for structural analyses.

Detailed finite element analyses of a fiber-matrix unit cell were performed using WYO2D [21] to characterize the nonlinear composite stress-strain behavior. WYO2D is a 2-D, generalized plane strain finite element analysis program developed by the Composite Materials Research Group in the Department of Mechanical Engineering at the University of Wyoming. It is specifically tailored for micromechanical analyses of continuous fiber-reinforced composite materials.

Transversely isotropic fiber properties and elastoplastic matrix properties were used in the micromechanical analyses. The plastic response of the matrix is initiated with an octahedral shear stress yield criterion, and governed by the Prandtl-Reuss flow rule which assumes that plastic strain is proportional to the deviatoric stress [22,23]. Matrix octahedral shear stress-strain behavior is developed from Richard-Blacklock curve fits of matrix solid rod torsion data at various temperatures and moisture levels.

A simplified unit cell model, developed by Pecknold [24], was chosen to approximate the micromechanical finite element analysis results and to interface to ABAQUS. The unit cell configuration is based on fiber and matrix "spring" elements in series and/or in parallel depending on the load path through these elements (see Figure 5). As in WYO2D, the fiber is considered transversely isotropic. In contrast to the elastoplastic matrix material model in WYO2D, the matrix shear behavior is nonlinear elastic and expressed in a Ramberg-Osgood form [25]. The fiber and matrix properties used in this model are listed in Tables 2 and 3. Stress averaging techniques are used to develop the response of the unidirectional lamina from the fiber-matrix unit cell. Unidirectional lamina are assembled into sublaminates (smallest repeating unit within the laminate) based on classical lamination theory and the condition that out-of-plane stresses at the layer interface must be continuous across the interface to satisfy equilibrium. The inhomogenous sublaminate is replaced by a homogeneous anisotropic material using equivalent continuum modeling

techniques.

Initial comparisons of the predicted in-plane shear response using the simplified unit cell model and WYO2D with matching matrix material models based on neat resin data showed that the simplified unit cell model predicted a stiffer response. The matrix material parameters in the simplified unit cell model were adjusted so that its predicted in-plane shear response matched WYO2D's for both AS4/3501-6 and S2 glass/3501-6 [20]. Figure 6 compares the predicted unidirectional composite through-thickness shear stress-strain behavior using WYO2D and the simplified unit cell model with the adjusted matrix material for AS4/3501-6 and S2glass/3501-6. There is good agreement between both predicted responses for AS4/3501-6, but the simplified unit cell model predicts a softer through-thickness shear response for S2 glass/3501-6. This effect has not been investigated, but may be related to the use of average rather than local stresses in the simplified unit cell model [24]. Figure 7 shows the predicted behavior for AS4/3501-6 and S2 glass/3501-6 crossply laminates using the simplified unit cell material model only. A composite laminate analysis is not possible with the micromechanical unit cell in WYO2D since it can be used to represent unidirectional composite geometries only. Since these curves represent the material response to a pure and uniform through-thickness shear loading, they are not necessarily expected to match the response generated with the V-notched beam specimen. The predicted material response is used in a finite element analysis of the specimen with its particular boundary and loading conditions, to generate the predicted response for the specimen.

Finite Element Model of the V-notched Beam Specimen

A 3-D finite element model was constructed following the dimensions of the V-notched beam specimen in Figure 2. Eight noded solid continuum brick elements (C3D8 in ABAQUS notation) were used throughout the model. The total number of elements was 250 with one element through the thickness. Maximum element aspect ratios were 3.6 or less for length:width and 6.25 or less for length:thickness.

Figure 2 also illustrates the boundary conditions applied to the model. On one side of the specimen, the nodes along the specimen edge in contact

with the fixture were fixed in the vertical direction. A vertical displacement was imposed on the other side. These are highly idealized boundary conditions. The effects of loading variations on solution results has been addressed for in-plane shear specimens by Morton [10], but will not be considered here.

Finite Element Computations

The simplified material model is interfaced to ABAQUS through a UMAT subroutine written by Hajali [26]. Strains are updated directly within the algorithm by adding the strain increment to the total strain at the previous increment. Both the total strain at the previous increment and the strain increment for the equivalent sublaminate material are supplied to the subroutine by ABAQUS. Micro level stress and strain increments are approximated using sublaminate stress and strain increments and tangent material properties in a reverse application of Pecknold's unit cell to sublaminate model described in the preceding section. The initial sublaminate stress increment will satisfy equilibrium and compatability, but not the nonlinear constitutive equations at the micro level. The stress increment is adjusted in an iterative process (modified Newton-Raphson method) until the constitutive conditions are satisfied to a specified tolerance. Future refinements of the stress update procedure are expected to improve computational speed and convergence time

In ABAQUS, a modified Riks algorithm was chosen to define the load on the specimen throughout the load step. This algorithm assumes proportional loading and that the load magnitude in each increment of the step is part of the solution rather than being specified by the user. Convergence within each increment was based on an acceptable tolerance measure for the solution of the equilibrium equations. ABAQUS recommends a tolerance measure two to four magnitudes less than typical nodal force values. Large displacement theory was used in the nonlinear analyses.

RESULTS

Experimental Results

Conventional Gages

Shear moduli as determined by back-to-back conventional gages, back-to-back full section gages and moiré/full section gages are listed in Table 1. Shear modulus was calculated by linear least squares regression of data between 1000 to 3000 (nominal) microstrain. Statistics are reported only on the modulus calculated using conventional gage results due to the limited number of specimens evaluated with the other strain measurement methods. A Student's *t* analysis [27] was used to compensate for the small sample size.

Ultimate shear strength is also reported in Table 1. Mean strengths are based on an average of specimens tested at NSWC using conventional gages and back-to-back full section gages. The single moiré/full section specimens tested at VPI&SU were not included in this average.

Moiré

Recordings of the U and V displacement fields in the test section of each of the four moiré specimens at specific applied average shear stress levels are shown in Figures 8 -11. The purity of shear in the test section is characterized by the lack of horizontal fringe gradients in the V field (ε_y) and lack of vertical fringe gradients in the U field (ε_x). Shear strain fields were relatively pure away from the notches for the graphite and glass crossplys and the glass unidirectional G_{23} specimen. Axial (ε_x) strains at the notch roots indicated the presence of in-plane bending possibly due to the low flexural stiffness of these specimens, particularly the unidirectional specimens. This is similar to findings by Morton et al. [10] for 90° (fiber orientation relative to the longitudinal axis of the specimen) graphite/epoxy in-plane shear V-notched beam specimens. The graphite/epoxy unidirectional G_{23} specimen exhibited the least pure shear behavior with significant axial strains in the test section. The glass/epoxy crossply specimen in Figure 11 exhibited some initial ε_x at the notch roots and flanks outside the test section. There was virtually zero normal strain in the test section as the load increased, until after

cracking of the notch roots/flanks occurred. Then significant ϵ_x and localized shear between plys became evident across the entire test section.

The shear strain distribution along the test section of each specimen was calculated from the moiré data, and is shown in Figures 12-15. The shear strain at each of the data points along the test section of the specimens has been normalized with the mean value of the shear strain for the moiré (front) side of those specimens. Distributions for all specimens were nonuniform, however, the crossplys exhibited more uniform behavior, away from the notch roots, than the unidirectional specimens.

Moiré/Full Section and Back-to-Back Full Section Gages

The average shear strain from the front (moiré) and the back (full section gage) of each specimen was averaged to determine the true average shear strain at several load levels. Plots for comparison of the moiré/full section data, back-to-back full section gages, and back-to-back conventional gages for unidirectional and crossply specimens of both material systems are shown in Figures 16 -17. Strain differences between the front and back of the specimen were observed at low load levels, but decreased with increasing load. This is consistent with observations by Morton et al. [10] for 0^o in-plane V-notched beam specimens which showed little sensitivity to twisting effects. For the unidirectional G_{23} specimens, the moiré/full section data and the back-to-back full section gage data are in excellent agreement. A localized lower stiffness on the order of 10-13% is calculated with the conventional gage data which does not account for the nonuniform strain distribution across the entire test section. A similar response is also apparent in the crossply graphite/epoxy specimens, especially beyond 0.7% strain. This effect is not as severe for the glass/epoxy crossply specimens, as indicated by the distributions (Figure 15) and the relatively good agreement between the moiré/full section data and the conventional gage data.

SEM

Photomicrographs of graphite and glass crossply failures are shown in Figure 18 (a) and (b) respectively. Shear cracks are apparent between 0^o and 90^o laminae and tensile cracks are apparent within the 90^o laminae. The AS4 specimens also showed some shear cracks within the 90^o laminae. Photographs of characteristic failures of the unidirectional specimens are shown in Figure 19. These failures are reminiscent of those observed in isotropic specimens as reported by Sullivan, Kao and Van Oene [28] and consistent with assumptions of transverse isotropy in the 2-3 plane.

Experimental/Analytical Results

Analysis Versus Conventional Gage Results

Analyses with linear and nonlinear elastic material properties are compared to data from the 062 back to back strain gages. Gauss point shear strains were obtained from the elements physically located beneath the strain gage. The corresponding shear stress was the average of the Gauss point shear stresses in the elements from notch root to notch root at the center of the specimen. Average shear stresses from the analysis were used in order to make a direct comparison with the experimental data where stresses were obtained by dividing the load by the cross-sectional area between the notches. Boundary conditions remained the same for analyses with both linear and nonlinear elastic material properites. No attempt was made to model the possibility of changing boundary conditions, particularly for the crossply specimens with measured strains near 3.5%.

Figure 20 shows predicted through-thickness shear stress-strain curves in the strain gage region for unidirectional AS4/3501-6 and S2 glass/3501-6. Only slight differences are observed between the linear and nonlinear elastic analyses. Agreement between analysis and data is excellent. Corresponding stress-strain curves for the cross-ply laminates are shown in Figure 21. Significant differences are observed between the linear and nonlinear responses beyond 1.5% strain for AS4/3501-6 and 1.0% strain for S2 glass/3501-6. The measured strains exceed those obtained from the analysis for S2 glass/3501-6 beyond 1.0% strain.

Analysis Versus Moiré/Full Section Gage Data

Comparisons to the moiré/full section gage results were made using both the average stresses and strains at the Gauss points of the elements from notch root to notch root in the specimen center. Analysis results using nonlinear elastic material properties agreed well with the available moiré/full section and back-to-back full section data points for unidirectional and crossply arrangements of both materials as shown in Figures 22 and 23. Additional moiré points in the nonlinear range were not obtained for the crossply laminates due to difficulty in fringe resolution at higher stress levels.

CONCLUSIONS

Through-thickness shear V-notched beam shear specimens have been investigated both experimentally and numerically to assess strain field uniformity and purity, and the effect of 3-D nonlinear vs. 3-D linear elastic material properites on finite element analysis results.

Crossply specimens of both AS4 and S2 glass exhibited uniform strain distributions away from the notches resulting in good correlation of conventional gages and moiré/full section gage data at low stress levels. Strain distributions in the AS4 and S2 glass unidirectional specimens peaked in the center of the specimen between the notches so that strains measured by conventional gages exceeded the average strain across the test section. This resulted in a lower modulus prediction with conventional gage data as compared to moiré/full section data. Significant axial strains existed in the test section of the unidirectional AS4 specimens, while the unidirectional S2 glass and crossply specimens of both materials showed fairly pure states of shear in the test section. No significant strain differences were observed between the front and back of the specimen.

Finite element analysis results using a 3-D nonlinear elastic material model correlated well with observed responses for all strain measurement methods. The use of linear elastic material properties resulted in a stiffer predicted response for the crossply specimens beyond 1% and 1.5% strain for S2 glass and AS4 respectively. The inclusion of nonlinear constitutive effects are recommended in the analysis of these specimens.

ACKNOWLEDGMENTS

The authors would like to express their appreciation to Drs. D. Post and P. Ifju (VPI&SU) for their assistance and guidance in the application of moiré interferometry techniques as required by this program. The authors would also like to thank Dr. J. Morton (VPI&SU) for his insights regarding specimen response, strain measurement techniques, and analysis procedures.

REFERENCES

1. Wilkins, D.J., "A Preliminary Damage Tolerance Methodology for Composite Structures," Workshop on Failure Analysis and Mechanisms of Failure of Fibrous Composites, NASA Langley Research Center, 1982.

2. Gillespie, J.W., "Damage Tolerance of Composite Structures: The Role of Interlaminar Fracture Mechanics," Journal of Offshore Mechanics and Arctic Engineering, September 1990.

3. Paul, P.C, C.R. Saff, K.B. Sanger, M.A. Mahler, H.P. Kan, and E.F. Kautz, "Out of Plane Analysis for Composite Structures," Eighth DOD/NASA/FAA Conference on Fibrous Composites in Structural Design, Norfolk, Virginia, 1989.

4. Serabian, Steve M., "The Effects of Nonlinear Intralaminar Shear Behavior on the Modeling Accuracy of $[(0/90)_3,0]_S$ and $[(+45/-45)]_{3S}$ Pin-Loaded Laminates," Journal of Composites Technology and Research, JCTRER, Vol. 13, No. 4, Winter 1991, pp.236-248.

5. Sumich, Mark and Keith K dward, "Development of a Fatigue-Life Methodology for Composite Structures Subjected to Out-of-Plane Load Components," NASA TM 102885, February 1991.

6. Martin, R.H. and W.C. Jackson, "Damage Prediction in Cross-Plied Curved Composite Laminates," NASA TM 104089, USAAVSCOM TR 91-B-009, July 1991.

7. Jones, Robert M., Mechanics of Composite Materials, McGraw-Hill Book Co., New York, 1975.

8. Lagace, P.A. and D.B. Weems, "A Through-the-Thickness Strength Specimen for Composites," Test Methods for Design Allowables for Fibrous Composites: 2nd Volume, ASTM STP 1003, C.C. Chamis, Ed., American Society for Testing and Materials, Philadelphia, 1989, pp. 197-207.

9. Walrath, D.E. and D.F. Adams, "The Iosipescu Shear Test as Applied to Composite Materials," Experimental Mechanics, 23 (1983), pp. 105-110.

10. Morton, J., H. Ho, and M.Y. Tsai, "An Evaluation of the Iosipescu Specimen for Composite Materials Shear Property Measurement," Journal of Composite Materials, 26 (1992), pp. 708-750.

11. Adams, D.F. and D.E. Walrath, "Current Status of the Iosipescu Shear Test Method," Journal of Composite Materials, 21 (1987), pp. 494-507.

12. Wilson, Dale W., "Evaluation of the V-notched Beam Shear Test Through and Interlaboratory Study," Journal of Composites Technology and Research, Vol. 12, No. 3, Fall 1990, pp. 131-138.

13. Kessler, Jeff A. and Donald F. Adams, "Composite Specimen Design Analysis - Volume II: Experimental Efforts - Appendix: Stress Strain Curves," U.S. Army Materials Technology Laboratory MTL TR 91-5, January 1991.

14. Ifju, P. and D. Post, "A Special Strain Gage for Shear Testing of Composite Materials," Proceedings SEM Spring Conference on Experimental Mechanics, Milwaukee, Wi. (1991).

15. Guo, Y. and P. Ifju, "A Practical Moire Interferometry System for Testing Machine Applications," Experimental Techniques, Vol. 15, No. 1, Jan/Feb. 1991, p. 29.

16. ASTM Specification D3171- 76, Test Method for Fiber Content of Resin-Matrix Composites by Matrix Digestion, ASTM Book of Standards, Vol. 15.03, 1990.

17. ASTM Specification D2584- 68, Test Method for Ignition Loss of Cured Reinforced Resins, ASTM Book of Standards, Vol. 8.02, 1990.

18. Post, D., "Moire Interferometry for Composites," Chapter 4, Manual on Experimental Methods for Mechanical Testing of Composites, M.E. Tuttle,

R.L. Pendleton, Eds., Society for Experimental Mechanics (1988).

19. Hibbitt, Karlsson, and Sorensen, "ABAQUS User's Manual," Version 4.7, Hibbitt, Karlsson,and Sorensen, Inc., Providence, R.I. (1988).

20. Gipple, K.L., "3-D Nonlinear Constitutive Modeling Approach for Composite Materials," CarderockDiv SME-92/25, May 1992.

21. WYO2D Finite Element Analysis Computer Program User Instructions and Documentation, Composite Materials Research Group, Mechanical Engineering Department, University of Wyoming, Laramie, Wyoming, November 1990.

22. Adams, D.F. and D.A. Crane, "Combined Loading Micromechanical Analysis of a Unidirectional Composite," Composites, July 1984, pp. 181-192.

23. Dieter, G.E., Mechanical Metallurgy, McGraw-Hill Book Co., New York, 1961.

24. Pecknold, D.A., "A Framework for 3-D Nonlinear Modeling of Thick-Section Composites," DTRC/SME-90-92, October 1990.

25. Ramberg, W. and W.R. Osgood, "Description of Stress-Strain Curves by Three Parameters," National Advisory Committee for Aeronautics, NACA, TN 902, July 1943.

26. Hajali, Rami, PhD Dissertation Work, University of Illinois at Urbana-Champaign, Department of Civil Engineering 1991.

27. Dally, J.W., W.F. Riley, and K.G. McConnell, Instrumentation for Engineering Measurements, John Wiley and Sons, Inc., New York, 1984.

28. Sullivan, J.L., B.G. Kao and H. Van Oene, "Shear Properties and a Stress Analysis Obtained from Vinly-ester Iosipescu Specimens," Experimental Mechanics, September 1984, pp. 223-231.

Orientation	Material	Strain Measurement Method	Number of Specimens	Modulus GPa (Msi)[1]	Strength MPa (Msi)[2]
Unidirectional G_{23} Specimens	AS4/3501-6	Conventional	3	2.81 (0.40) 1.5%	32.45 (4.65) 7.2%
		Moire/Full	1	3.14 (0.45)	
		Back-to-Back Full	2	3.14 (0.45)	
	S2 glass/3501-6	Conventional	3	6.29 (0.90) 13.9%	39.75 (5.69) 13.7%
		Moire/Full	1	6.99 (1.00)	
		Back-to-Back Full	2	7.05 (1.01)	
Crossply Specimens	AS4/3501-6	Conventional	4	3.91 (0.56) 2.3%	91.37 (13.06) 1.9%
		Moire/Full	1	3.91 (0.56)	
		Back-to-Back Full	2	3.91 (0.56)	
	S2 glass/3501-6	Conventional	4	6.22 (0.89) 3.8%	90.89 (13.01) 4.0%
		Moire/Full	1	5.24 (0.75)[3]	
		Back-to-Back Full	2	6.36 (0.91)	

NOTES:

1. Statistics computed only for specimens with conventional gages. Numbers in per cent (for both modulus and strength) indicate accuracy with a reliability of 95% based on a Student *t* analysis to compensate for the small sample size [27].
2. Mean strength is based on an average of strengths obtained from specimens with conventional gages and back-to-back full section gages. All these specimens were tested in the same fixture at NSWC.
3. Only two moire points at low load levels were available for modulus calculations. Typically, as the load was increased, the discrepancy between front (moire) and back (full section gages) decreased. Modulus based on full section gages alone is 6.45 GPa (0.92 Msi).

Table 1 Out-of-plane shear modulus and strength values for unidirectional and crossply AS4/3501-6 and S2 glass/3501-6 laminates

PROPERTY	FIBER	
	AS4	S2GLASS
E_1 (GPa)	224	88
E_2 (GPa)	14	88
E_3 (GPa)	14	88
ν_{12}	.2	.22
ν_{13}	.2	.22
ν_{23}	.25	.22
G_{12} (GPa)	14	35
G_{13}(GPa)	14	35
G_{23}(GPa)	5.6	35

Subscripts indicate direction

1 Along fiber

2,3 Transverse to fiber

Table 2 AS4 graphite and S2 glass fiber properties used in analysis

Property	Epoxy Resin 3501-6 Room Temperature, 0% Moisture
K (GPa)	2.0
G (GPa)	1.9
β	1.0
N	5.0
τ_0 (MPa)	106

Bulk Modulus

$K = E / (9 - 3 E / G)$

Ramberg Osgood Shear Model

$$\gamma = \tau/G + \beta(\tau_0/G)(\tau/\tau_0)^N$$

τ Shear stress

γ Shear strain

G Initial tangent shear modulus

β, N, τ_0 Curvature parameters

Table 3 3501-6 epoxy matrix properties used in simplified unit cell model

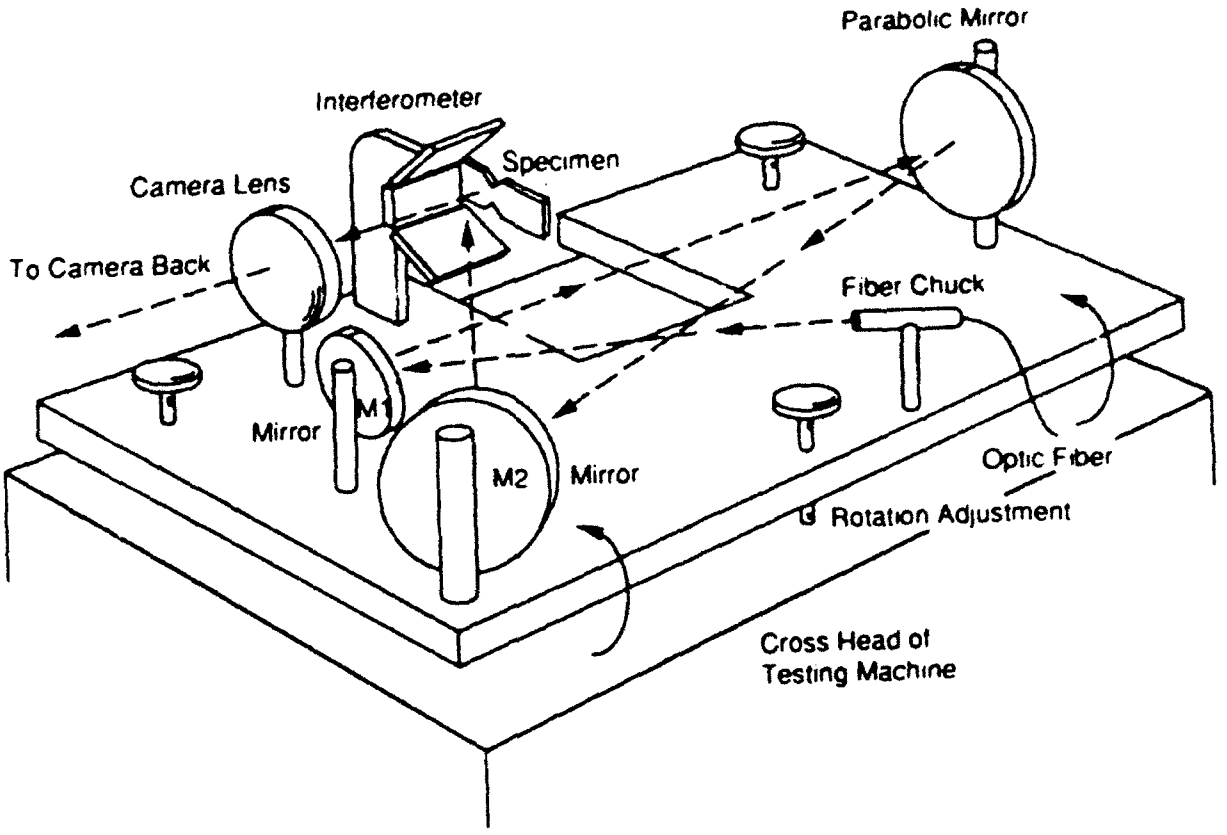

Figure 1 Schematic of moiré setup after Guo and Ifju [15]

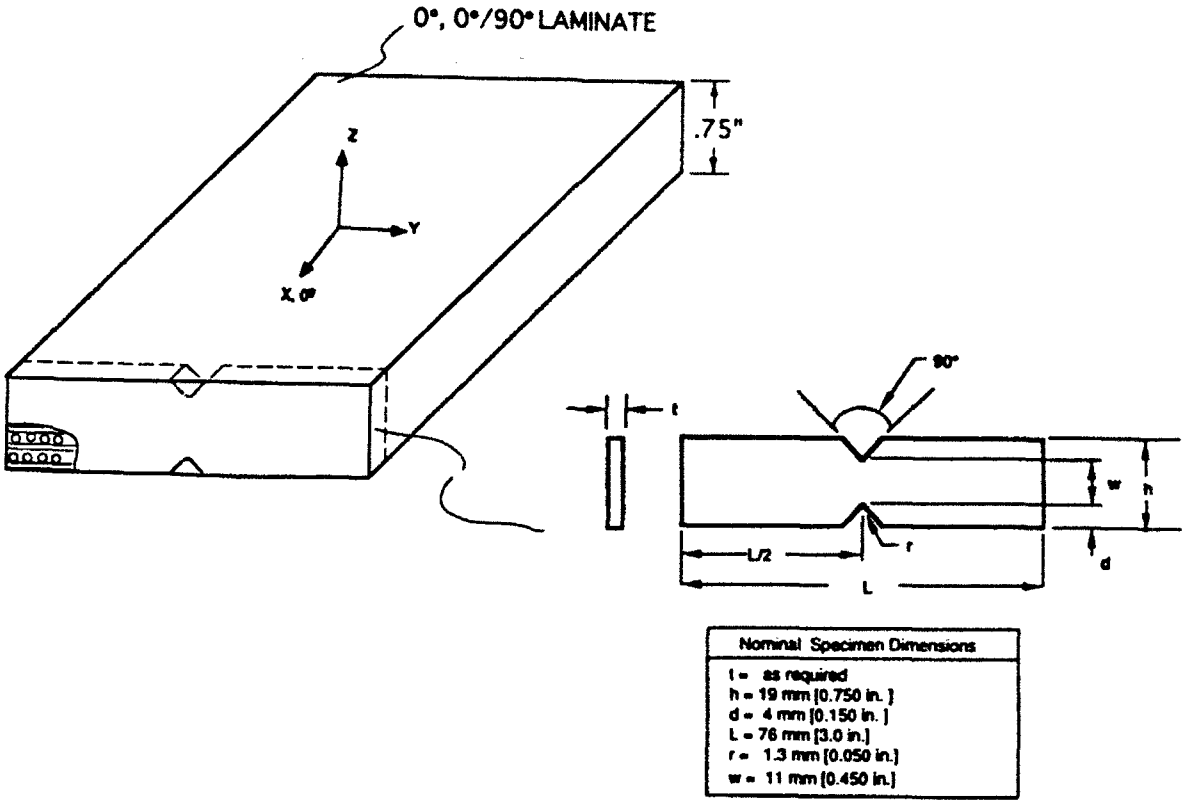

(a) Specimen orientation and geometry

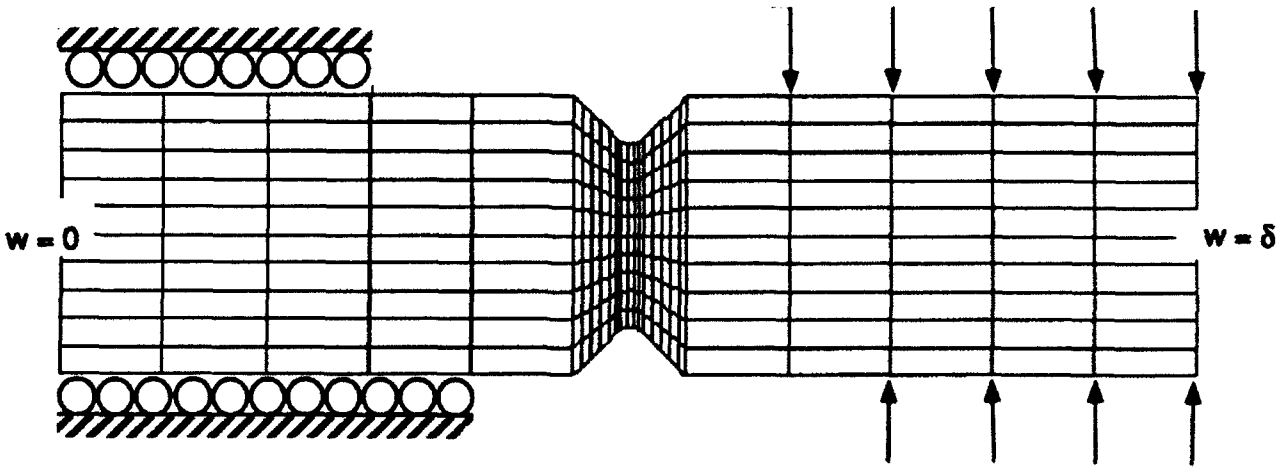

(b) Finite element mesh and boundary conditions

Figure 2 V-notched beam specimen (a) specimen orientation and geometry, (b) finite element mesh and boundary conditions

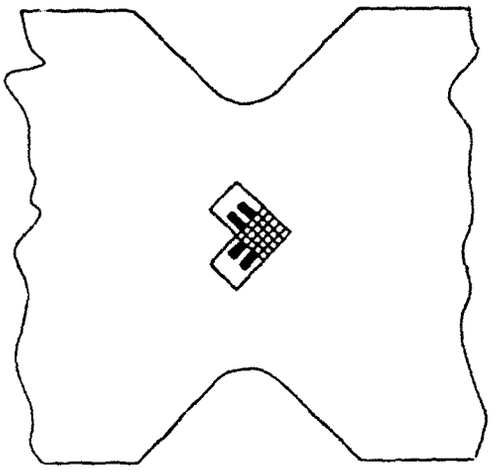

(a)

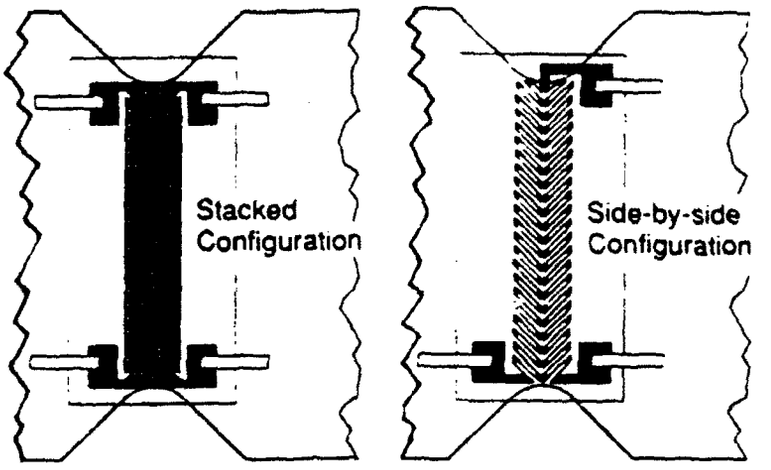

(b)

Figure 3 Strain gages used in study (a) conventional 0/90 stacked gage, (b) full section gages in stacked and side-by-side configurations

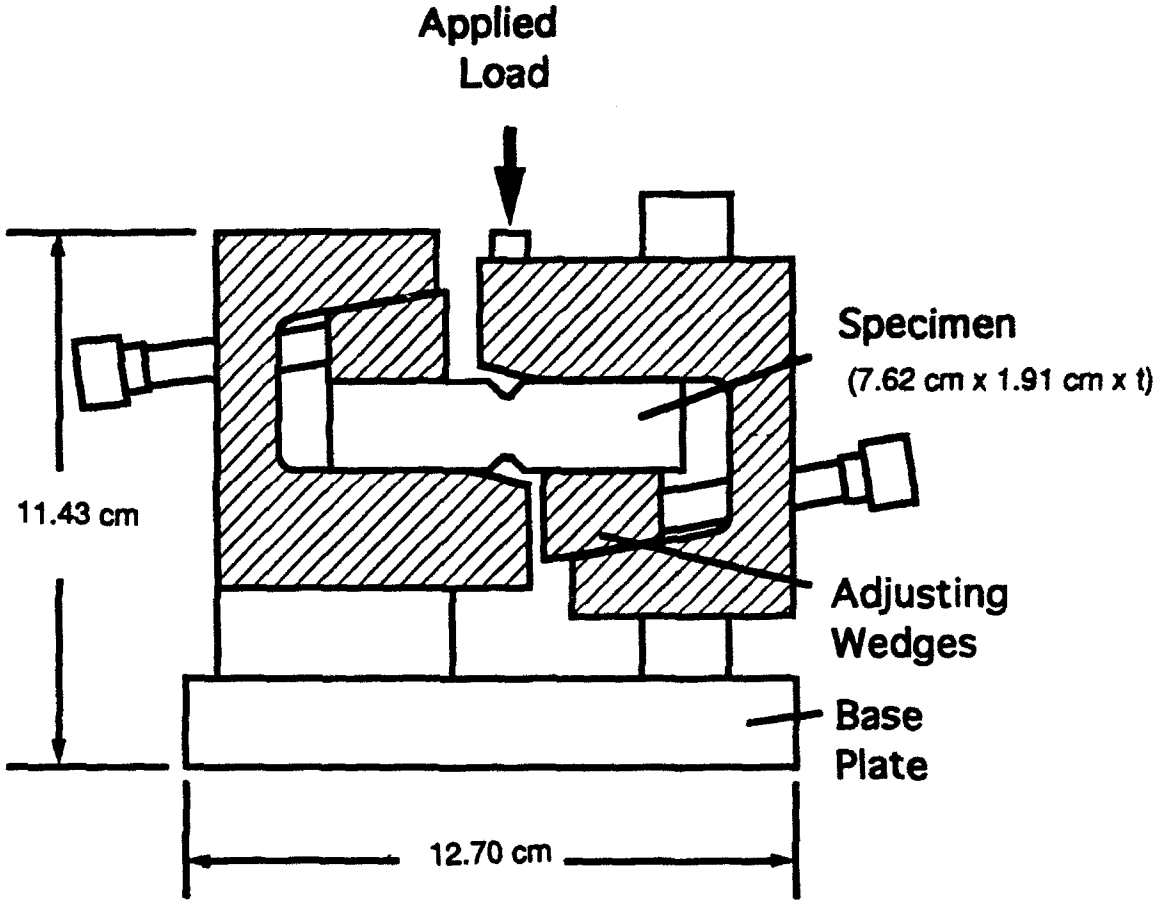

Figure 4 V-notched beam test specimen mounted in test fixture modeled after fixture developed by Adams and Walrath [9]

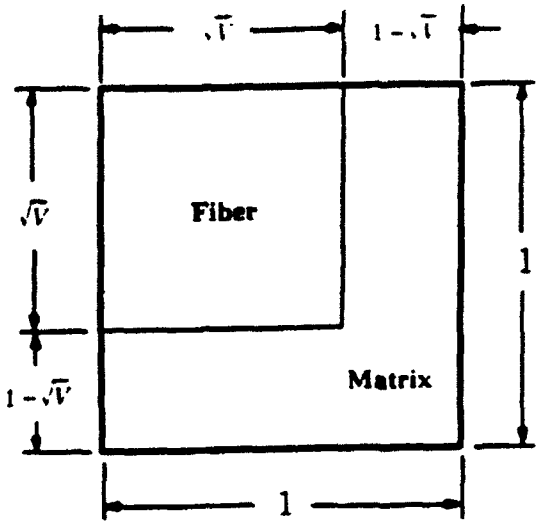

Unit Cell (V = Fiber Volume Fraction)

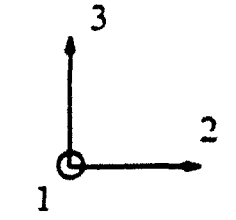

1 = Fiber Direction

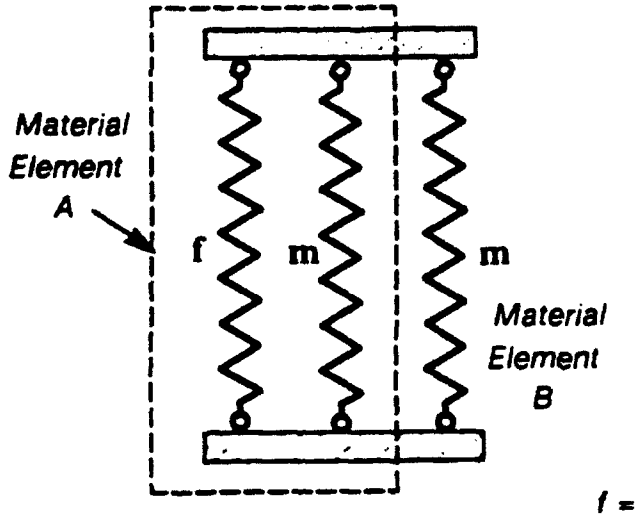

f = fiber
m = matrix

For component 11

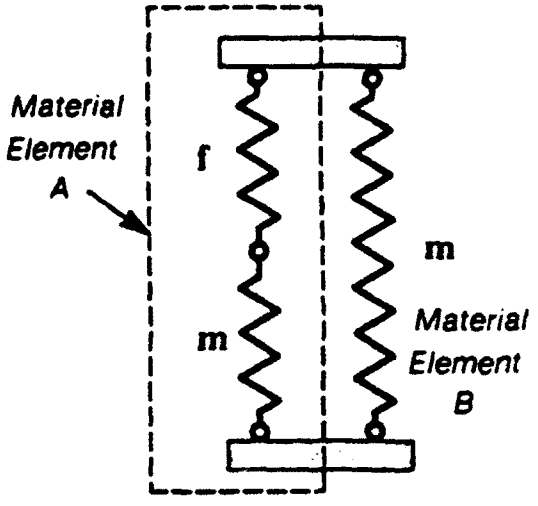

For components
22, 12, 33, 23, 13

Figure 5 Simplified unit cell model based on spring analogy showing the load path variations between fiber and matrix dominant components [24]

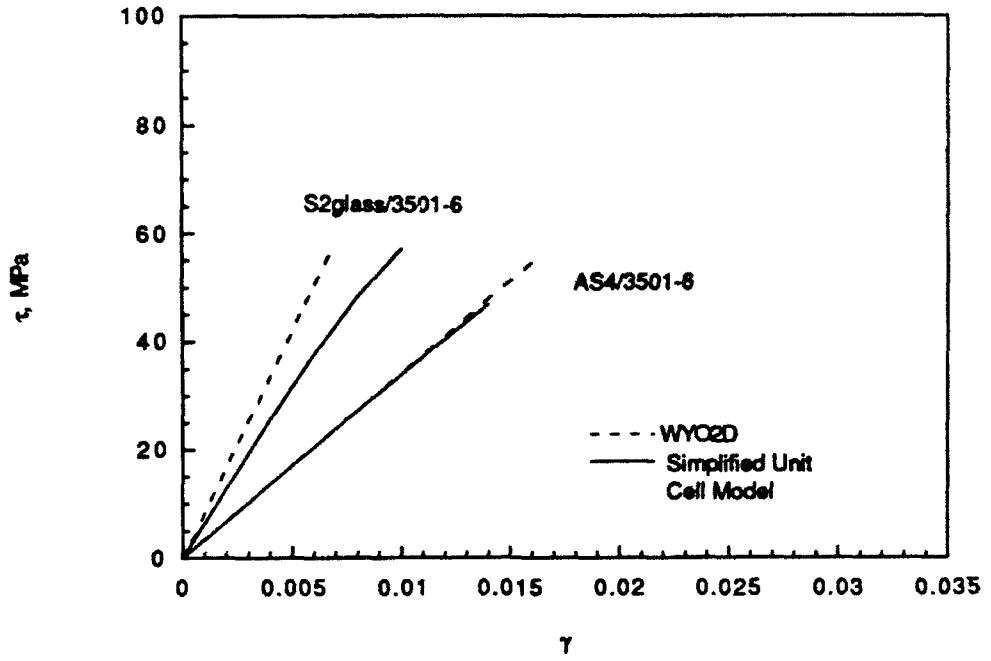

Figure 6 Predicted through-thickness shear behavior for unidirectional (G_{23}) AS4/3501-6 and S2 glass/3501-6 using WYO2D and the simplified unit cell model

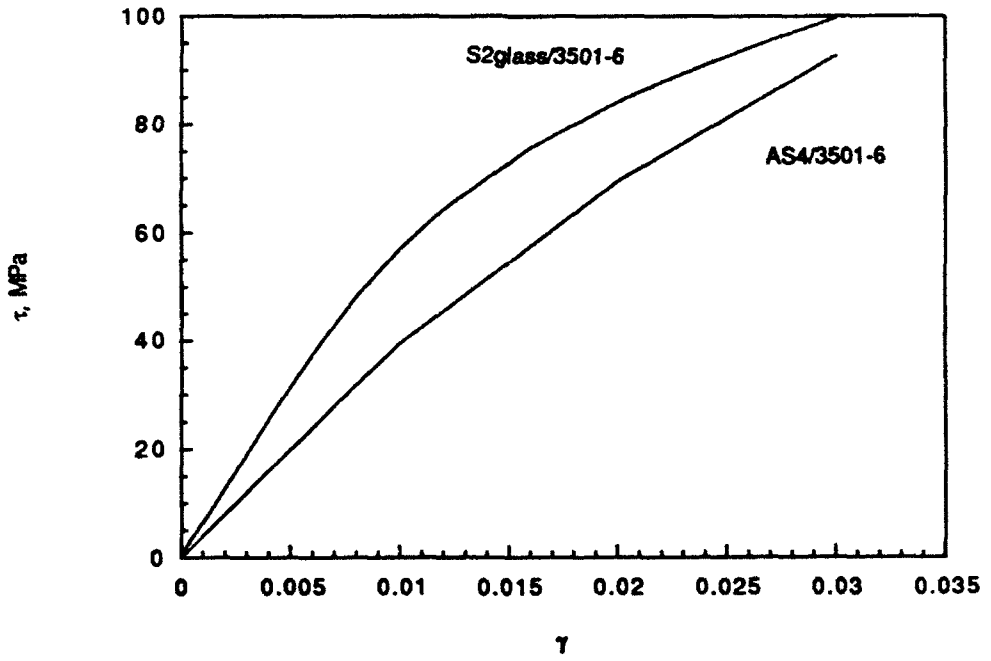

Figure 7 Predicted through-thickness shear behavior for AS4/3501-6 and S2 glass/3501-6 crossply laminates using the simplified unit cell model

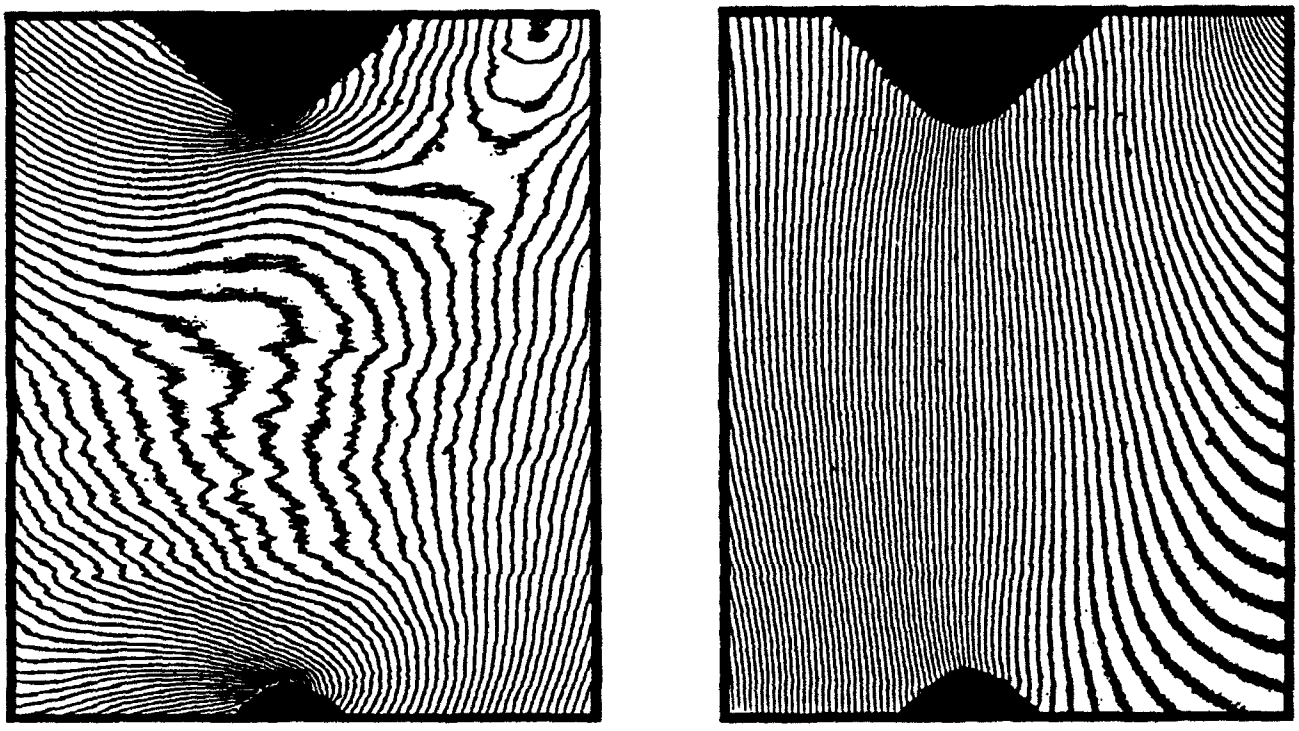

(a) (b)

Figure 8 U (a) and V (b) moiré field fringe patterns for unidirectional (G_{23}) AS4/3501-6 specimens loaded at 23 MPa and 7.7 MPa respectively

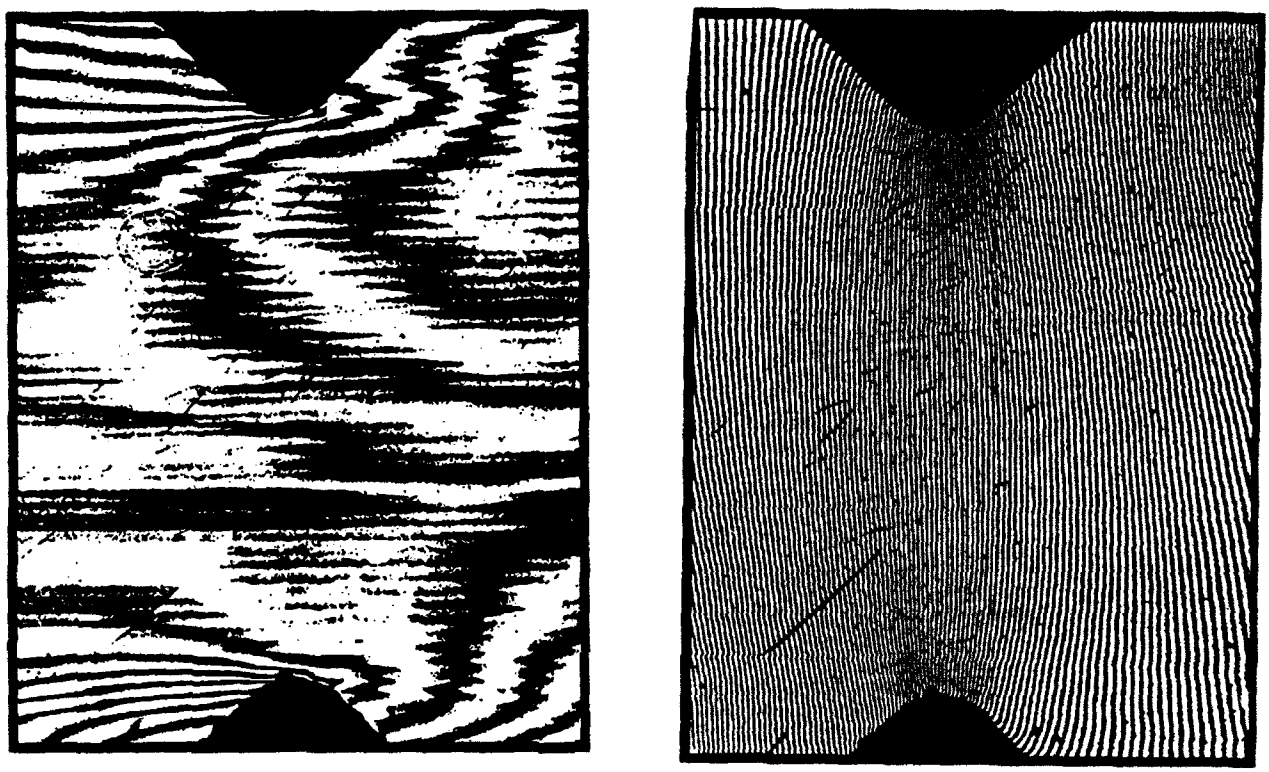

(a) (b)

Figure 9 U (a) and V (b) moiré field fringe patterns for AS4/3501-6 crossply specimen at a load level of 14.3 MPa

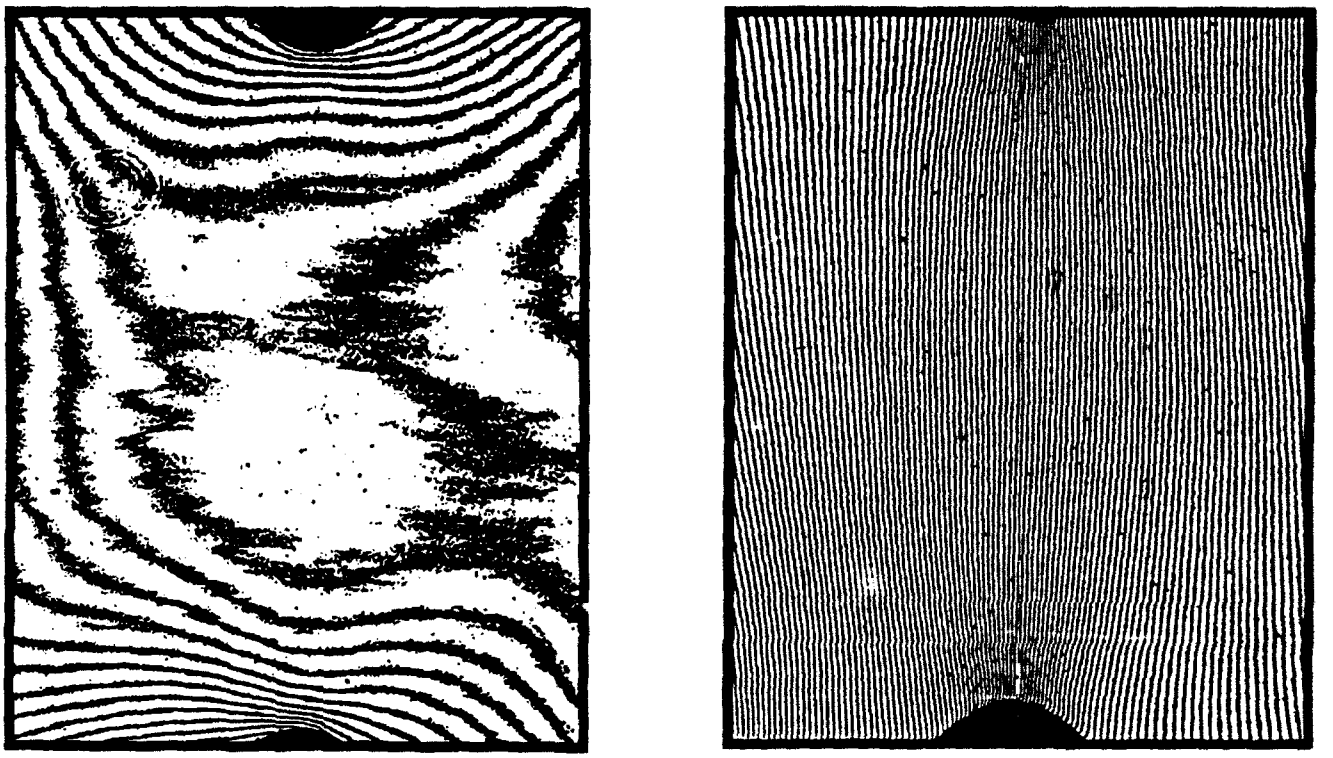

(a) (b)

Figure 10 U (a) and V (b) moiré field fringe patterns for unidirectional (G_{23}) S2 glass/3501-6 specimens loaded at 21 MPa

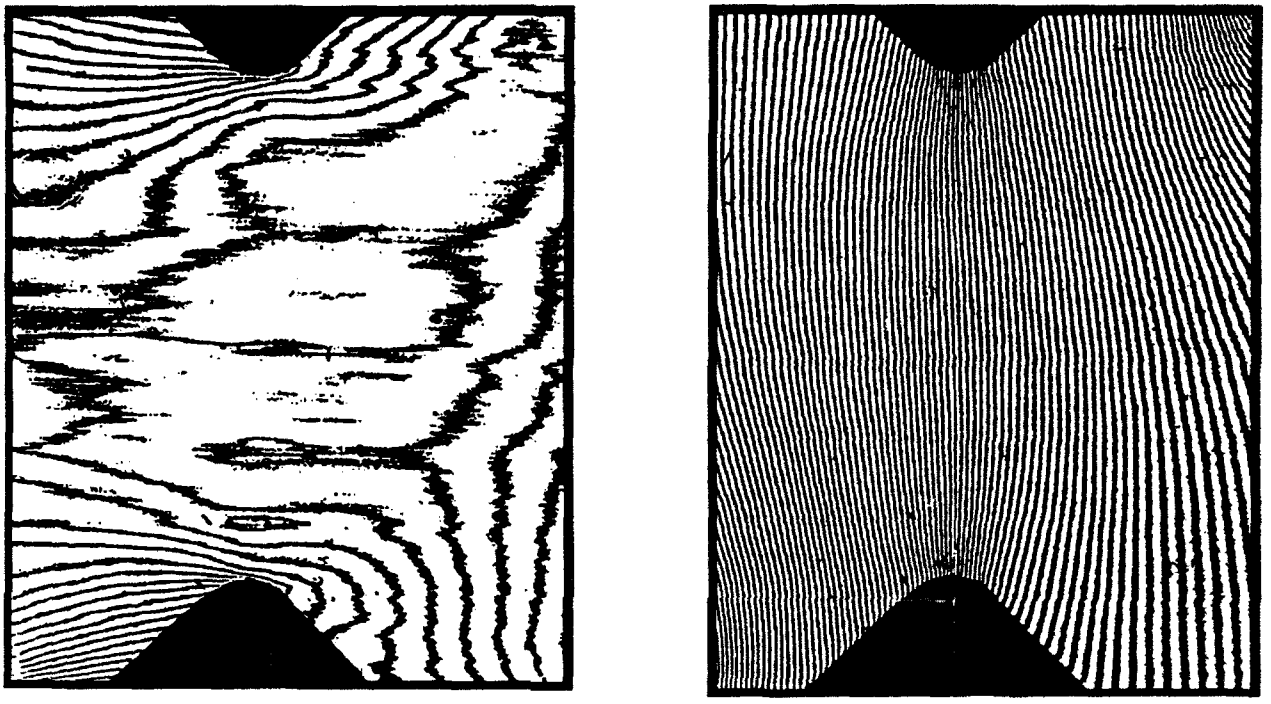

(a) (b)

Figure 11 U (a) and V (b) moirė field fringe pattterns for S2 glass/3501-6 crossply specimens loaded at 21.8 MPa and 11.3 MPa respectively

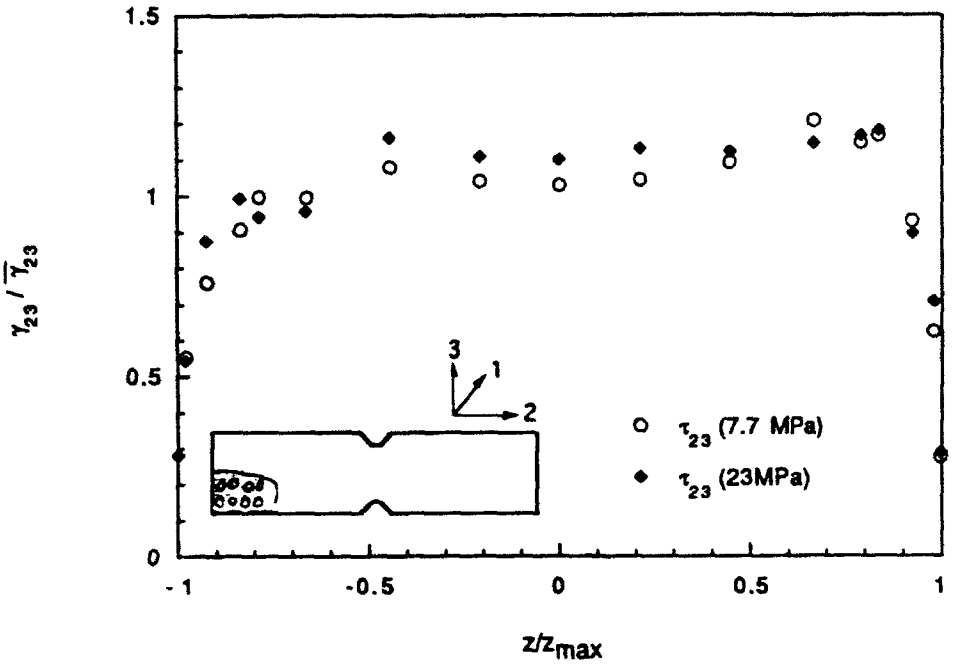

Figure 12 Normalized shear strain distribution along the test section of a unidirectional (G_{23}) AS4/3501-6 V-notched beam specimen measured by high sensitivity moiré at two load levels

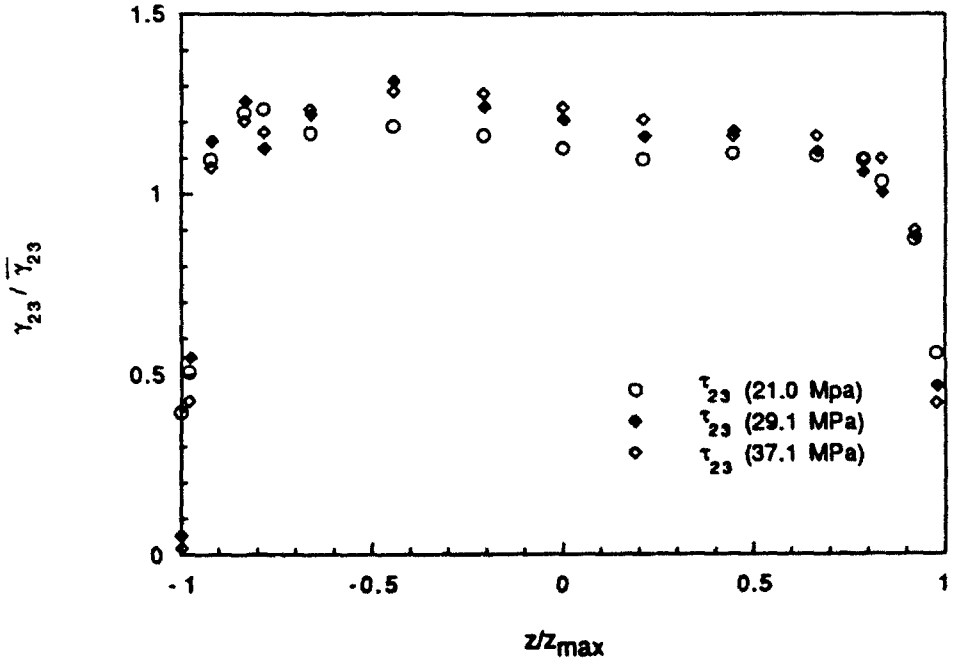

Figure 13 Normalized shear strain distribution along the test section of a unidirectional (G_{23}) S2 glass/3501-6 V-notched beam specimen measured by high sensitivity moiré at several load levels

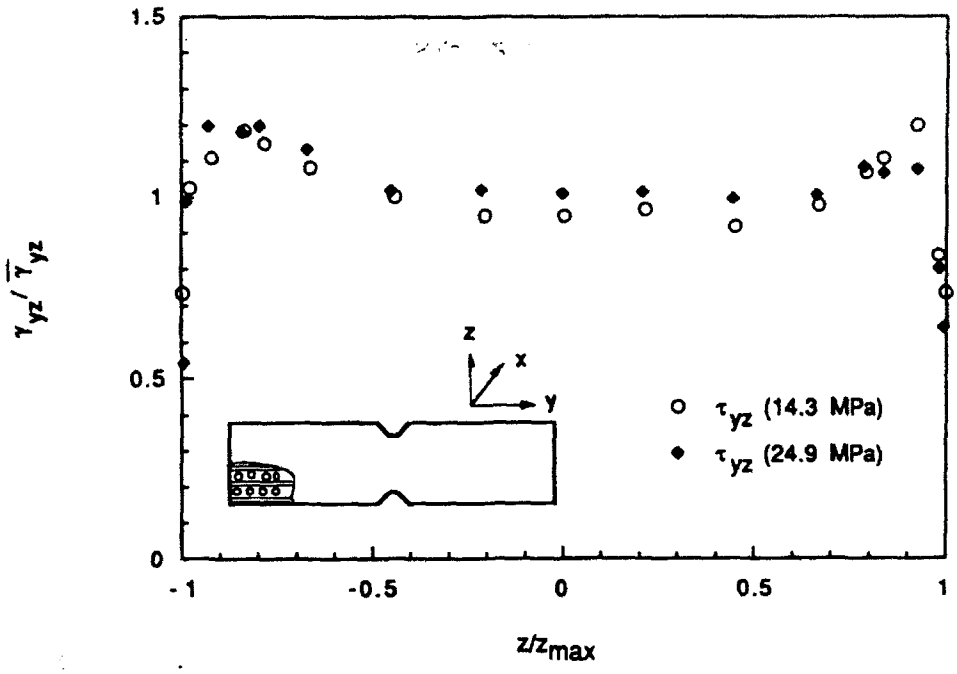

Figure 14 Normalized shear strain distribution along the test section of a crossply AS4/3501-6 V-notched beam specimen measured by high sensitivity moiré at two load levels

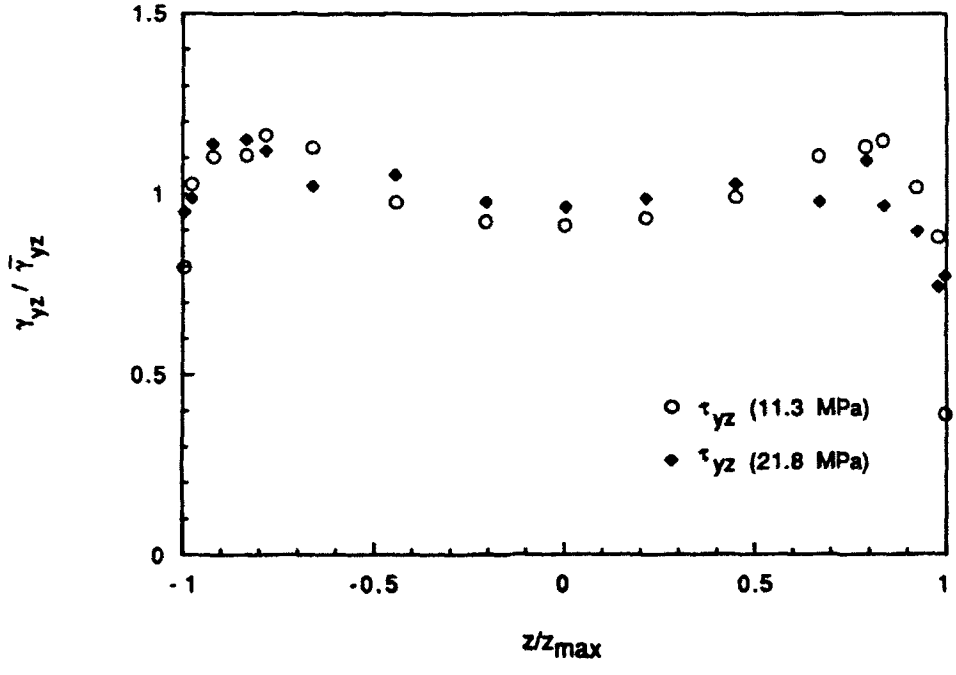

Figure 15 Normalized shear strain distribution along the test section of a crossply S2 glass/3501-6 V-notched beam specimen measured by high sensitivity moiré at two load levels

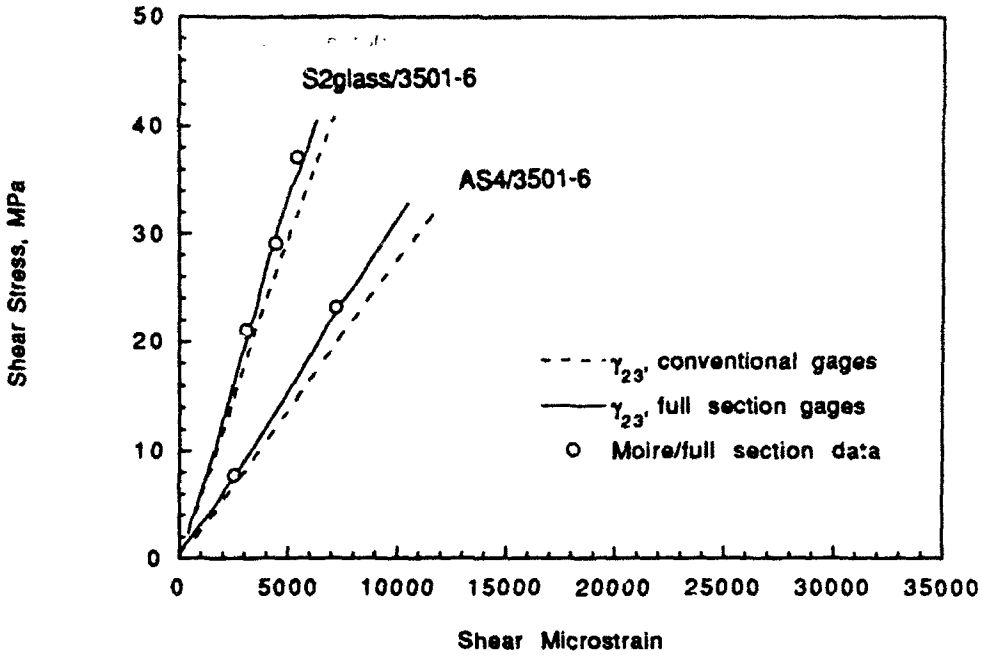

Figure 16 Shear stress-strain response for AS4/3501-6 and S2 glass/3501-6 unidirectional (G_{23}) specimens instrumented with conventional gages vs. moiré and full section gage data

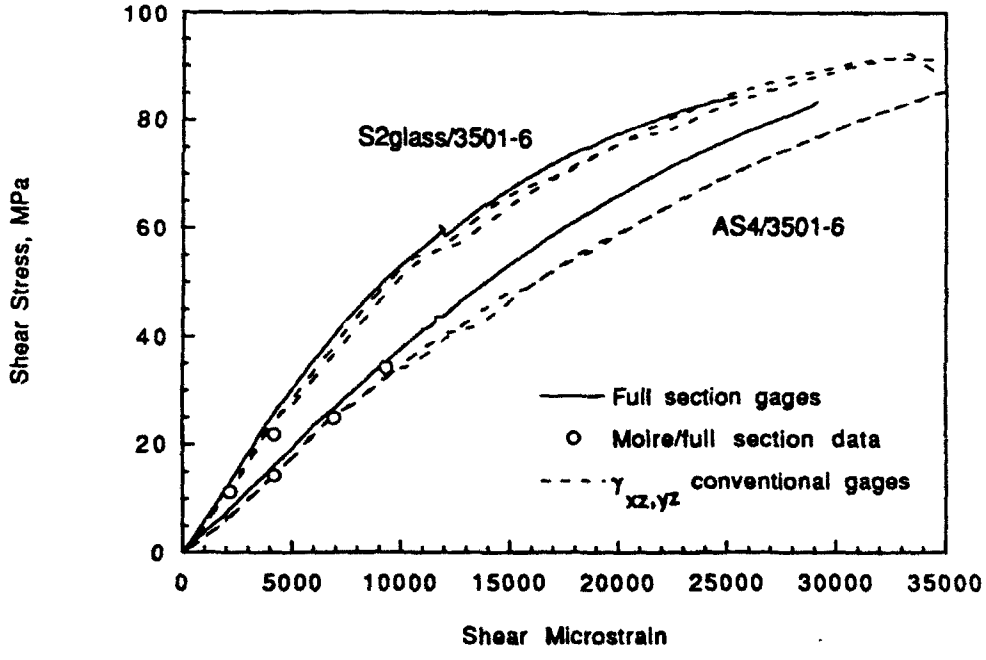

Figure 17 Shear stress-strain response for AS4/3501-6 and S2 glass/3501-6 crossply specimens instrumented with conventional gages vs. moiré and full section gage data

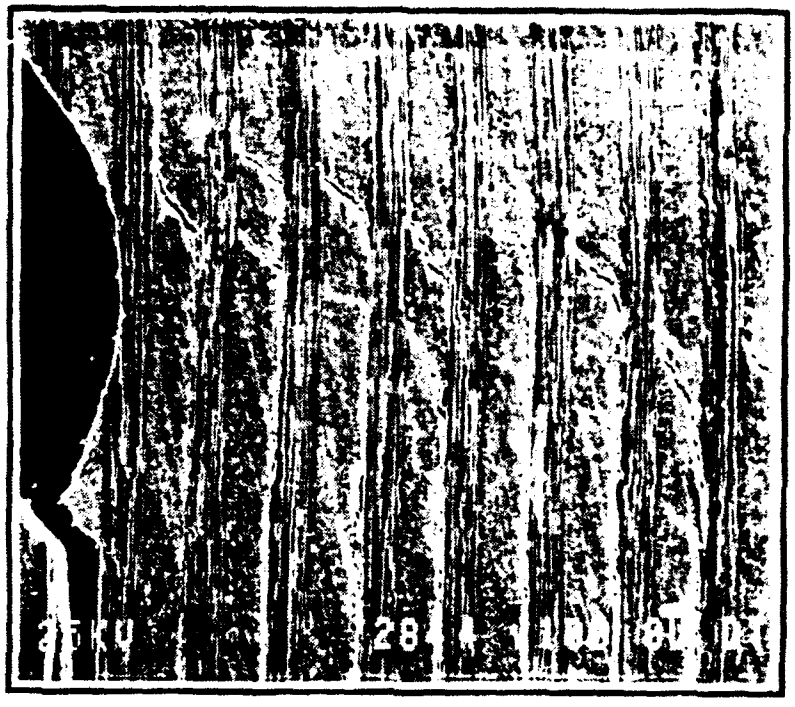

(a) AS4/3501-6

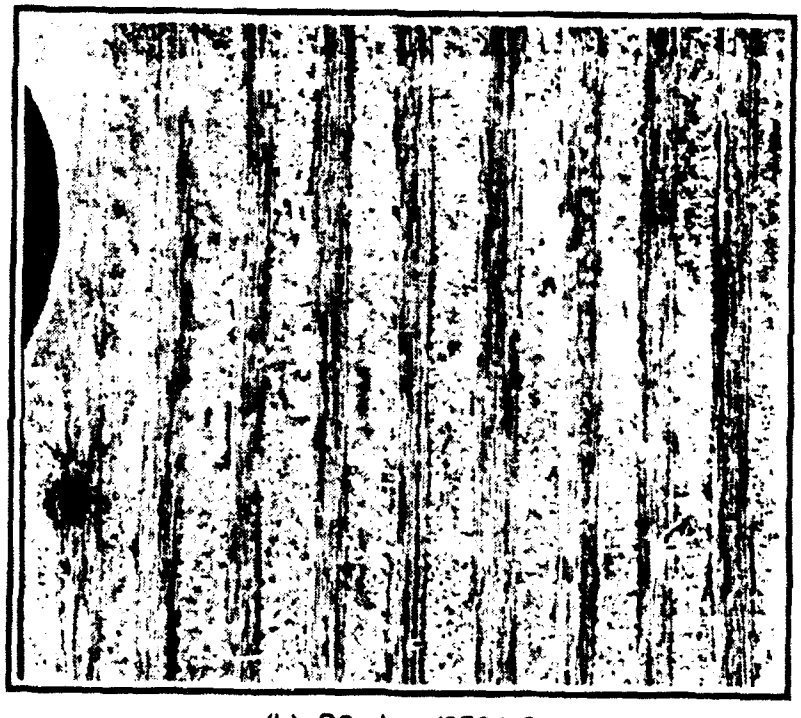

(b) S2 glass/3501-6

Figure 18 Photomicrographs of AS4/3501-6 and S2 glass/3501-6 crossply specimen failures

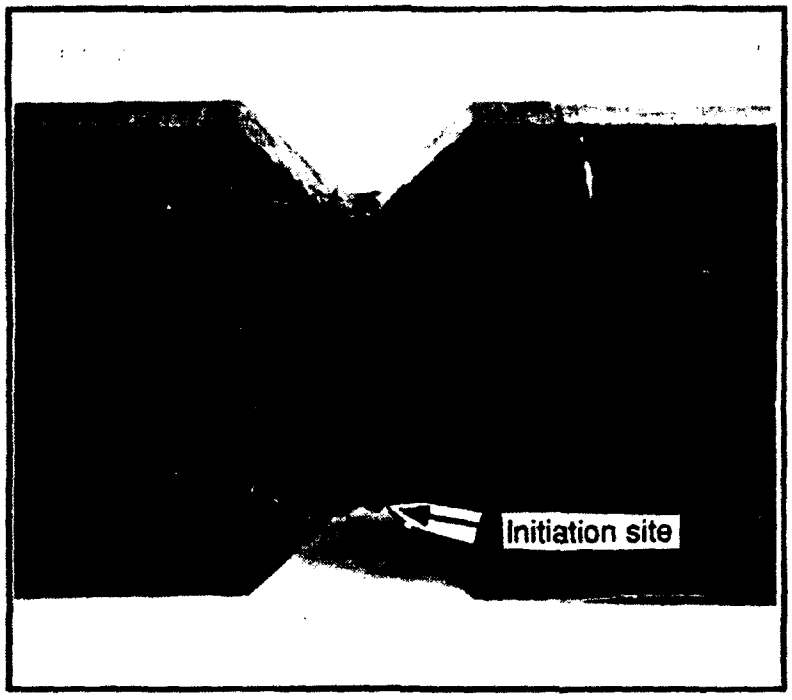

(a) AS4/3501-6

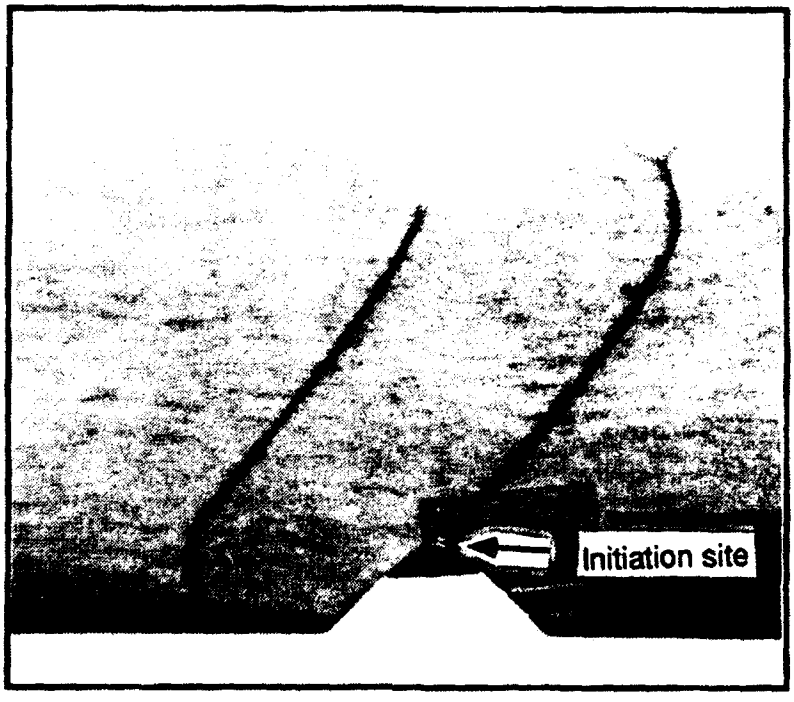

(b) S2 glass/3501-6

Figure 19 Photographs of AS4/3501-6 and S2 glass/3501-6 unidirectional specimen failures

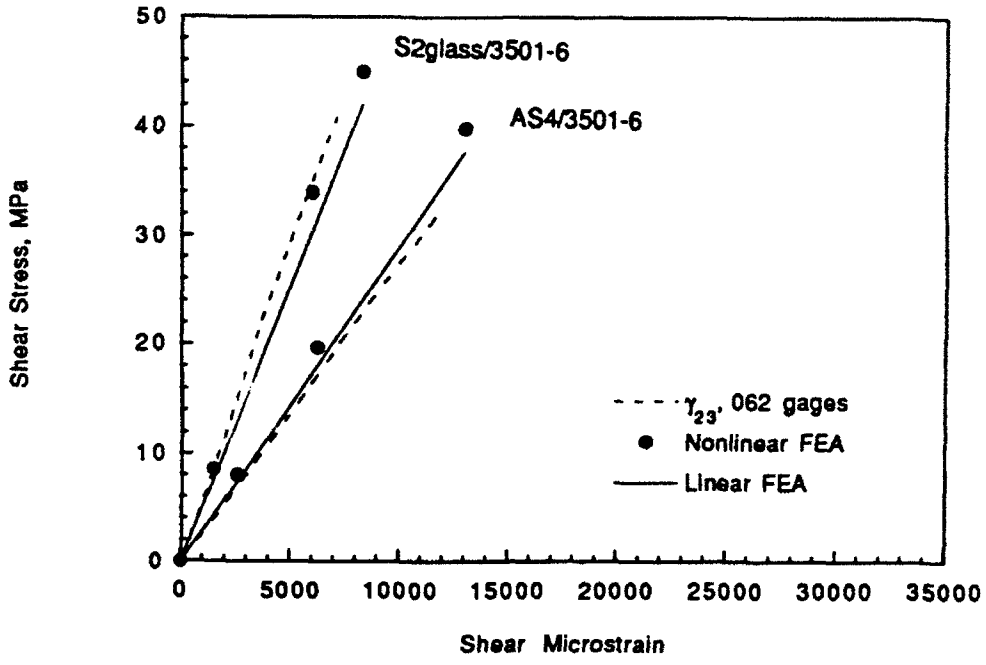

Figure 20 Shear stress-strain response for unidirectional (G_{23}) AS4/3501-6 and S2 glass/3501-6 specimens instrumented with conventional gages (062) vs. predicted values based on finite element analyses with linear and nonlinear elastic material properties

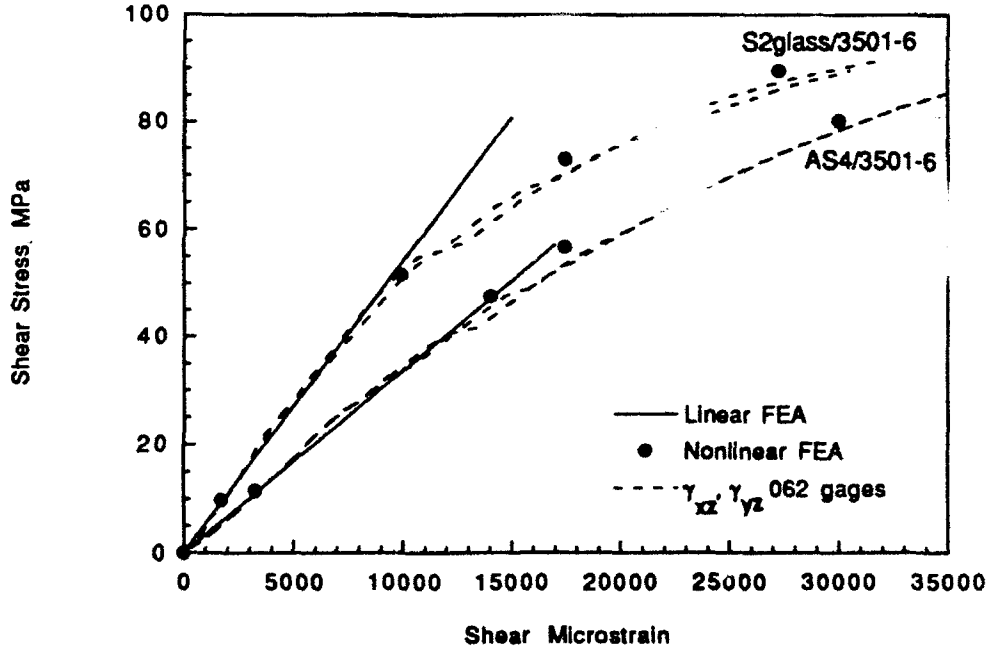

Figure 21 Shear stress-strain response of crossply specimens predicted by finite element analyses with linear and nonlinear elastic material properties, and measured by conventional (062) gages

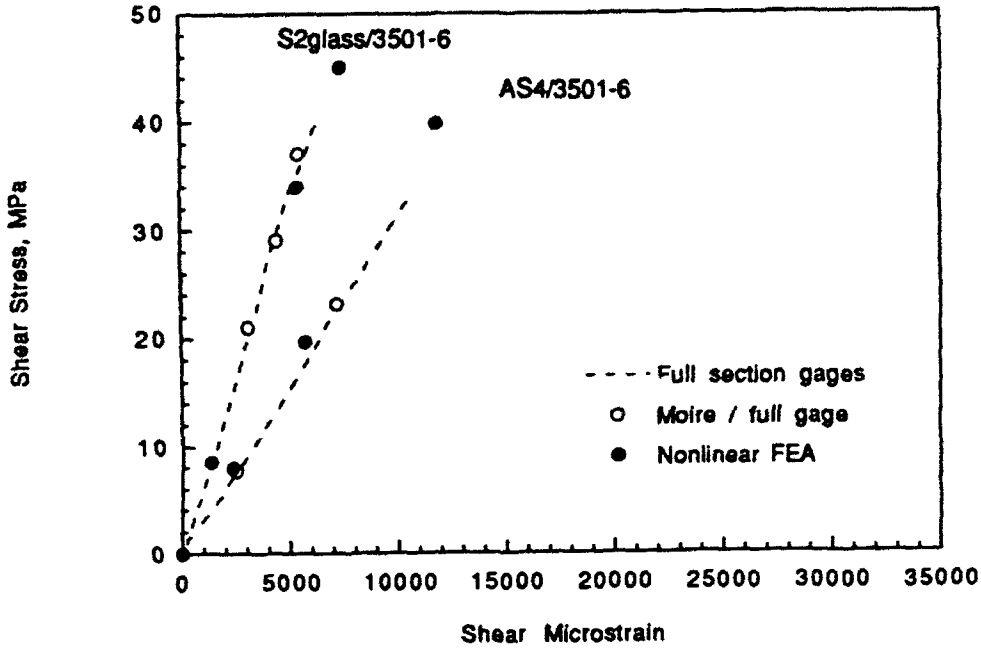

Figure 22 Average shear stress-strain response for AS4/3501-6 and S2 glass/3501-6 unidirectional (G_{23}) specimens measured with moiré interferometry and full section gages vs. predicted values based on finite element analyses with nonlinear elastic material properties

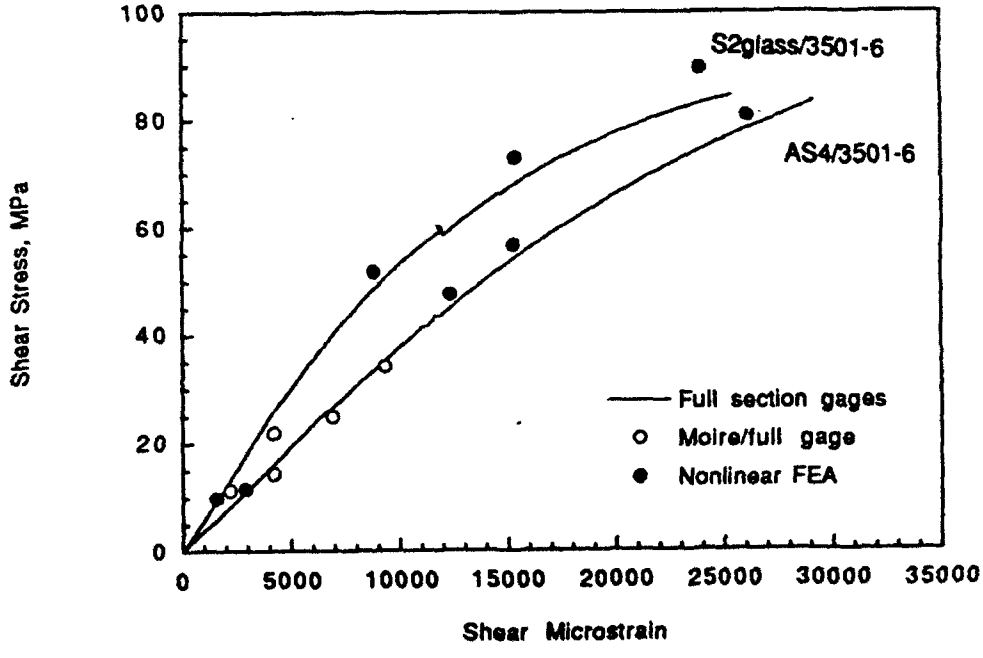

Figure 23 Average shear stress-strain response for AS4/3501-6 and S2 glass/3501-6 crossply specimens measured with moiré interferometry and full section gages vs. predicted values based on finite element analyses with nonlinear elastic material properties

Copies

4 DTIC

4 ONR
1 1132SM (Rajapakse)
1 1131S (Fishman)
1 1132SM (Barsoum)
1 1216 (Vasudevan)

1 ONT
1 233 (Remmers)
1 225 (Sloter)

1 DARPA - MSTO
1 (Kelly)

3 NAVSEA
1 05M3 (Pinto)
1 55Y2 (McCarthy)
1 55Y2 (Will)

2 PEO-SUB
1 R (Troffer)
1 R (Spero)

3 NRL
1 6380 (Badaliance)
1 6383 (Wolock)
1 6385 (Chaskelis)

1 NSWC
1 R31 (Augl)

2 University of Illinois at Urbana-Champaign
Dept. of Civil Engineering
Urbana, Ill. 61801
2 (Dr. Dave Pecknold)

1 McDonnell Aircraft Company
Thermoplastic Composites Development
Building 102, Level 2W, MC1021310
James S. McDonnell Blvd.
Berkeley, Mo. 63134
1 D356 (Ray Bohlmann)

1 Hercules
Bracchus Works
P.O. Box 98
Magna, Ut. 84044
1 (Dr. Ralph Nuismer)

1 Engineering Science and Mechanics Department
Virginia Polytechnic Institute
and State University
Blacksburg, Va. 24061
1 (Dr. John Morton)

1 General Dynamics Electric Boat Div.
75 Eastern Point Road
Groton, Ct. 06340
1 443/J11-431 (Dr. Jeff Hall)

CENTER DISTRIBUTION

Copies	Code	Name
1	0115	Caplan
1	0113	Douglas
1	17	Krenzke
1	1702	Corrado
1	172	Rockwell
1	176	Sykes
2	1720.2	Phyillaier
		Bonanni
1	1720.4	Wiggs
1	1730.2	Critchfield
1	2723	Wilhelmi
1	274	Wang
1	28	Wacker
2	2801	Morton
2	2802	Camponeschi
		Crane
1	2803	Cavallaro
1	281	Holsberg
1	283	Singerman
1	284	Fischer
1	2844	Castelli
10	2844	Gipple
1	3422	TIC Annapolis
2	3431	Office Services

REPORT DOCUMENTATION PAGE

Form Approved
OMB No. 0704-0188

1. AGENCY USE ONLY (Leave blank)	2. REPORT DATE	3. REPORT TYPE AND DATES COVERED
	October 1992	RD&E 10/90-9/92

4. TITLE AND SUBTITLE
Measurement of the Out-of-Plane Shear Response of Thick Section Composite Materials Using the V-notched Beam Specimens

5. FUNDING NUMBERS
Program Element:62234N
Task No: R3450S0S

6. AUTHOR(S)
K.Gipple and D.Hoyns

7. PERFORMING ORGANIZATION NAME(S) AND ADDRESS(ES)
Naval Surface Warfare Center
Carderock Division
Annapolis Detachment
Code 2844/644

8. PERFORMING ORGANIZATION REPORT NUMBER
CRDKNSWC-SSM-64-92/22

9. SPONSORING /MONITORING AGENCY NAME(S) AND ADDRESS(ES)
Office of Naval Technology
Materials Block

10. SPONSORING /MONITORING AGENCY REPORT NUMBER

11. SUPPLEMENTARY NOTES

12a. DISTRIBUTION /AVAILABILITY STATEMENT
Approved for public release; distribution is unlimited.

12b. DISTRIBUTION CODE

13. ABSTRACT *(Maximum 200 words)*

The out-of-plane shear response of thick, unidirectional and crossply, AS4/3501-6 and S2 glass/3501-6 laminates was investigated theoretically and experimentally. The specimens considered were of the V-notched beam (Iosipescu) configuration. Strains were monitored in the specimen test sections using conventional strain gages, moire interferometry, and new full section strain gages. Crossply laminates exhibited a fairly uniform strain distribution away from the notches resulting in agreement of initial moduli obtained through all three strain measurement methods. Strains measured with conventional gages centered between the notches of the unidirectional specimens exceeded the average strain from notch to notch, as measured by moire interferometry and the full section data. Measured strains correlated very well with predicted strains from specimen finite element analyses using nonlinear elastic material properties.

14. SUBJECT TERMS
Composite materials, nonlinear behavior, transverse shear, graphite/epoxy, glass/epoxy

15. NUMBER OF PAGES

16. PRICE CODE

17. SECURITY CLASSIFICATION OF REPORT	18. SECURITY CLASSIFICATION OF THIS PAGE	19. SECURITY CLASSIFICATION OF ABSTRACT	20. LIMITATION OF ABSTRACT
UNCLASSIFIED	UNCLASSIFIED	UNCLASSIFIED	Same as report